A Globally Efficient Means of Distributing UTC Time & Frequency Through GPS

John A. Kusters, Robin P. Giffard and Leonard S. Cutler
Hewlett–Packard Co.
David W. Allan, Allan's TIME
Mihran Miranian, U.S. Naval Observatory

Abstract

Time and frequency outputs comparable in quality to the best laboratories have been demonstrated on an integrated system suitable for field application on a global basis. The system measures the time difference between 1 pulse–per–second (pps) signals derived from local primary frequency standards and from a multi–channel GPS C/A receiver. The measured data is processed through optimal SA Filter algorithms that enhance both the stability and accuracy of GPS timing signals.

Experiments were run simultaneously at four different sites. Even with large distances between sites, the overall results show a high degree of cross–correlation of the SA noise. With sufficiently long simultaneous measurement sequences, the data shows that determination of the difference in local frequency from an accepted remote standard to better than 1×10^{-14} is possible. This method yields frequency accuracy, stability, and timing stability comparable to that obtained with more conventional common–view experiments. In addition, this approach provides UTC(USNO MC) in real time to an accuracy better than 20 ns without the problems normally associated with conventional common–view techniques.

An experimental tracking loop was also set up to demonstrate the use of enhanced GPS for dissemination of UTC(USNO MC) over a wide geographic area. Properly disciplining a cesium standard with a multi–channel GPS receiver, with additional input from USNO, has been found to permit maintaining a timing precision of better than 10 ns between Palo Alto, CA and Washington, DC.

Introduction

Because GPS provides time traceable to Coordinated Universal Time (UTC), and its rate is syntonized with the international definition of the second, it provides a world–wide resource for time and frequency with heretofore unprecedented accuracies and precisions.

Although selective availability (SA) limits navigation and position accuracy to slightly better than the 100 meter specification, a method of filtering the SA noise has been developed for timing during the past year. This method provides enhanced GPS (EGPS) operation[1]. The EGPS approach has been shown to provide a real–time UTC(USNO MC) with stabilities of a few nanoseconds and frequency stabilities of 1×10^{-14}. The EGPS timing technique is a systems approach. The quality of the output will depend on the clock used with the receiver.

An EGPS clock based on a high quality quartz oscillator has demonstrated timing stabilities of 20 ns rms, long–term frequency stability of better than 1×10^{-13}, and elimination of frequency drift and reduction of environmental effects on the system output[1].

GPS timing is becoming extremely important to society and to science. Major users include the Bureau International des Poids et Mesures (BIPM), which provides the standard for time and frequency, UTC; 45 national timing centers; NASA JPL's Deep Space Network; the world–wide measurement of the rapid–spin rates of the millisecond pulsars; NIST's global time service; NASA's timing of space platforms; and numerous other calibration and timing laboratories.

Of the six different methods of using GPS for timing[2], three are the most popular. These are GPS direct, EGPS, and GPS Common–View. Of these, EGPS has by far the best performance/cost ratio.

GPS common–view requires that the clock sites participating use single satellites according to a pre–arranged schedule and exchange data. A different approach (EGPS) will yield essentially the same data almost in real–time, but with a simplified procedure. A multi–channel GPS receiver approach permits looking at all satellites in view. Even at continental distances, common satellites are viewed most of the time. Thus, a high degree of correlation can be expected, even with sites on opposite sides of a continent. Rather than using a single satellite for a relatively short period of time and sharing raw data to determine frequency and time changes, EPGS uses proper processing of data from all available satellites to obtain time comparison between the local site and UTC(USNO MC), as broadcast by GPS. The frequency of the remote clock can be compared directly with the broadcast value of UTC(USNO MC) or with similar data received directly from USNO. These comparisons have accuracy uncertainties of 10^{-14}, or less than 10^{-14}, respectively.

Long integration times require the use of clocks that exhibit sufficient long–term stability to maintain stable time and frequency. Presently, commercially available primary cesium–beam frequency standards exhibit typical accuracy of $\approx 2 \times 10^{-13}$, long–term stability (better than 1×10^{-14} beyond 1 week), with minimal environmental sensitivity.[3] A feature of these standards is that they operate as steerable clocks. The output time and frequency can be controlled by known amounts so that they agree with an external reference. These clocks may be ensembled together to improve robustness of the system.[4] The ensemble output can be shown to be better than the best physical clock in the system. Reliability is enhanced since the system continues uninterrupted with only some loss in performance should any one of the clocks fail.

Timing signals are now available from the full GPS constellation of 24 or more satellites offering world–wide, multiple satellite timing information referenced to UTC(USNO MC) with a high level of redundancy, reliability, and robustness. In addition, low–cost commercial multi–channel GPS C/A receivers with 1 pps outputs are available.

SA Filtering

Until now, a significant problem with using GPS has been the imposition of Selective Availability (SA). SA is an intentional modulation added to the satellite clock signal such that a non–secure receiver cannot achieve full dynamic position accuracy. The recent development of effective,

optimal, SA filtering techniques based on the spectral characteristics of SA permits receiving UTC(USNO MC) time as broadcast by GPS almost as if SA were not present.[5]

These techniques provide no assistance in determining dynamic positioning, but are a major enhancement in determining time and frequency. Since UTC(USNO MC) is currently steered to UTC within ±60 ns, and the broadcast correction from GPS has a documented accuracy of about ±20 ns with respect to UTC(USNO MC), the system described provides a real–time access to UTC. Accurate measured values of the time difference between UTC (via GPS) and UTC(USNO MC) are available after a 48 hour delay. These can be used to improve further the timing accuracy to better than 10 ns.

Experimental Results: Part I

During April and May 1994, time difference data were taken at four sites. These were: the US Naval Observatory (USNO), Washington, DC, the National Institute of Standards and Technology (NIST), Boulder, CO, Hewlett–Packard Laboratories (HPL), Palo Alto, CA, and the Hewlett–Packard Santa Clara Division (SCD), Santa Clara, CA.

At each site, the same, low–cost commercially available, 6–channel GPS C/A timing receiver was installed. The time difference between the 1 pps signal derived from the GPS receiver and the 1 pps from the local primary frequency standard was measured using conventional time–interval measurement techniques. Used in this experiment were: the Master Clock at USNO, the output from Microstepper B (tied to UTC(NIST) at NIST, a single HP5071A cesium–beam frequency standard at HPL, and an active ensemble of three HP5071A standards at SCD.

No attempt was made to synchronize the GPS 1 pps signals to the local signals. The receiver time delays were not calibrated, but as all receivers were identical, a reasonable assumption is that the delays were approximately the same. Finally, except for USNO, no attempt was made to correct for all of the known fixed time delays either in the GPS antenna or in the 1 pps delay from the local standard. As a result, the data obtained can be used to determine frequency accuracy, frequency stability, time stability, but not time accuracy between the various sites.

The experimental results are shown in Figures 1 through 4. Each plot presents 300 second averaged data for each data point, since 300 seconds was the shortest common measurement time of the four sites involved. At three of the sites, data points were taken every second, then 100 consecutive values were averaged and the 1 second data discarded. At the fourth site, 1 second data points were averaged every 60 seconds. Also shown as a white line in each plot are the SA filtered data, obtained by post–processing the original experimental data with the SA filter algorithm. The mean value has been subtracted from all data in the plots. The SA filter algorithm used was such that in an on–line system, the same outputs could be obtained in real time.

The filtered data in Figure 1 was compared with the output of a secure two–frequency keyed GPS receiver. This receiver used the measured rather than the broadcast value for the ionospheric delay correction. The rms of the time difference between the filtered estimate and the secure receiver was 1.5 ns.

The improvement in time–domain stability obtained through the use of this optimum filtering routine is shown in Figure 5. The upper line shows the modified Allan Deviation (MDEV) of the NIST time difference data before filtering. The data are dominated by SA noise, and the slope is about -3/2, indicating a white–phase noise process. The lower line is the MDEV of the filtered NIST data. The amplitude of the noise has been reduced to approximately the noise level expected of a cesium standard. At 200,000 seconds, outside the stop–band of the SA filter, the value of MDEV observed is of the same order as the noise of the UTC–corrected GPS. The improved time domain stability is obtained at the cost of a longer response time.

Table 1 presents some of the experimental results obtained after all data have been corrected for constant frequency offsets and slopes. The correction factors are shown. Significant is an almost 500–fold improvement in time–domain stability at 300 seconds and the uniformity from site to site.

A close examination of the data in Figures 3 and 4 (HPL and SCD) indicates a high degree of correlation. Given that the two sites are less than 25 km apart, this is not unexpected since both sites see the same GPS satellites at essentially the same time. A difference plot of the data is shown in Figure 6. As the data for the four sites share a common binning scheme, the cross–correlation coefficients were calculated for several selected pairs over the period of common data bins between the sites. The results are shown in Table 2. As expected, correlation decreases with distance between observation sites. This is undoubtedly due to differences in the tropospheric and ionospheric correction factors and a decreasing number of satellites common to both sites.

Experimental Results: Part II

An experimental GPS tracking loop was set up to demonstrate the use of EGPS for dissemination of UTC(USNO MC) at a slightly improved accuracy over that from Part I. The experiment consisted of steering a cesium clock at Hewlett–Packard Laboratories in Palo Alto CA using the output of a multi–channel GPS receiver. The effects of the GPS–to–UTC(USNO MC) time–difference, and un–modelled receiver delays were minimized by using the readings from an identical receiver at USNO in Washington, DC the output of which was compared with the USNO master clock.

In order to avoid uncertainties due to the broadcast GPS to UTC(USNO MC) corrections, which could be as large as 100 ns, both receivers operated in the "GPS" timing mode.

At USNO the 1 pps output of a 6–channel receiver in the "position–hold mode" was timed with reference to UTC(USNO MC). Average time differences were computed using data extending over two days, evenly weighted. The averages were assigned to the modified Julian date (MJD) corresponding to the center of gravity of the data, and placed in a computer data file which could be read by ftp over Internet. The data file was automatically copied daily by the computer at HPL that managed the tracking loop. On receipt, the data in the file was usually between one and two days old.

At HPL the 1 pps output of an identical receiver in the same operating mode was compared with the 1 pps output of an HP 5071A cesium standard. Each hour, the readings taken in the

preceding 60 minutes were averaged and placed in a data file. A second–order feedback loop was used to steer the cesium standard. The inputs to the feedback calculation were the averaged time difference between the local clock and the output of the GPS receiver, and the averaged, delayed, data from USNO. The USNO data was processed by a simple predictor to estimate the current value of the GPS–UTC(USNO MC) time–difference. This value was subtracted from the local time difference and used to calculate a proportional frequency correction for the cesium standard.

The USNO data was subtracted from corresponding 2–day averages of the local time differences and summed into an integral that was scaled to give the frequency correction for the cesium standard. Effectively, over 90% of the 1 pps pulses at each site were used in the algorithm in order to minimize SA and quantization noise in the receiver. A block diagram of the tracking system is shown in Figure 7.

Initial operation of the tracking loop extended over 40 days. No independent check on the system accuracy with comparable resolution was available, so the results were analyzed on the basis of self–consistency. Figure 8 shows a histogram of the local two–day time differences, with the USNO two–day averages subtracted. The distribution is acceptable, with an rms value of 4 ns. This data shows the tracking error and is not affected by noise at frequencies lower than the loop cut–off, or noise that is coherent at both locations. This noise level compares quite well with the estimate of the cesium standard noise given by $\tau * \sigma_y(\tau)$ calculated for 2 days, which is 3.5 ns. The noise in the tracking loop is shown in Figure 9, which shows the Allan deviation calculated for the frequency corrections applied each 6 hours to the cesium standard. The deviations are compatible with the noise expected from the cesium standard, when the loop transfer function is taken into account. At 4 days the Allan deviation of the frequency corrections is 1.5×10^{-14}. This represents the rms total of the cesium standard noise and the noise introduced by the GPS tracking loop including SA.

This performance suggests that excellent results can be obtained with time–tracking loops using multi–channel GPS receivers, even in the presence of SA. For good time resolution, a high quality local clock is essential. The performance of the loop described could be improved by better algorithms for estimating the real–time GPS–UTC(USNO MC) difference, and for minimizing diurnal effects in the GPS data. The performance of this loop will also depend on the dynamics and magnitude of the GPS–UTC(USNO MC) time difference, which was comparatively small during this experiment.

Summary

The full set of data indicates that the EGPS technique permits a stable local clock to be steered accurately to UTC(USNO MC) using the GPS timing signal. The experimental results indicate that over a one month time period, frequency transfer accuracies of a few $\times 10^{-15}$ are possible. Although no attempt was made to correct for fixed time delays in these experiments, it appears that sufficient accuracy can be obtained to maintain a local time scale close to the performance limits of the GPS system if the system delays are carefully determined.

Acknowledgments

The authors sincerely acknowledge the active assistance of personnel from the United States Naval Observatory, and Victor Zhang and Marc Weiss of the Time and Frequency Division of the National Institute of Standards and Technology.

References

[1] J.A. Kusters, et.al., *"A No–drift and less than* 1×10^{-13} *Long–term Stability Quartz Oscillator Using a GPS SA Filter,"* Proceedings of the 1994 IEEE International Frequency Control Symposium, IEEE Catalog No. 94CH3446–2, pp. 572–577, June 1994.

[2] D.W. Allan, et.al., *"Civil GPS Timing Applications,"* presented at the 1994 ION GPS–94 Conference, Salt Lake City, Sept. 1994.

[3] J.L. Johnson and J.A. Kusters, *"A New Cesium Beam Frequency Standard — Performance Data,"* Proceedings of the 1992 IEEE Frequency Control Symposium, IEEE Catalog No. 92CH3083–3, pp. 143–150, June 1992

[4] S.R. Stein, *"Advances in Time Scale Algorithms,"* Proceedings of the Precise Time and Time Interval Applications and Planning Meeting, NASA Conference Publication 3218, pp. 289–302, Dec. 1992.

[5] D.W. Allan and W.P. Dewey, *"Time–Domain Spectrum of GPS SA,"* Proceedings of the ION GPS–93, Sixth International Technical Meeting of the Satellite Division of the Institute of Navigation.

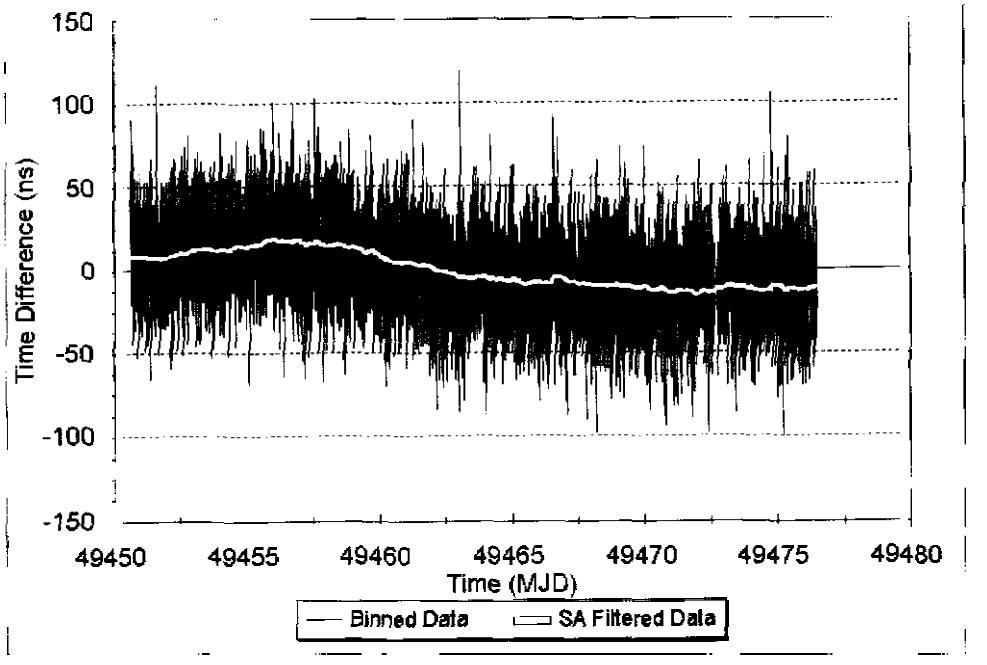

Figure 1. GPS vs. USNO Master Clock -- 300 second binned data

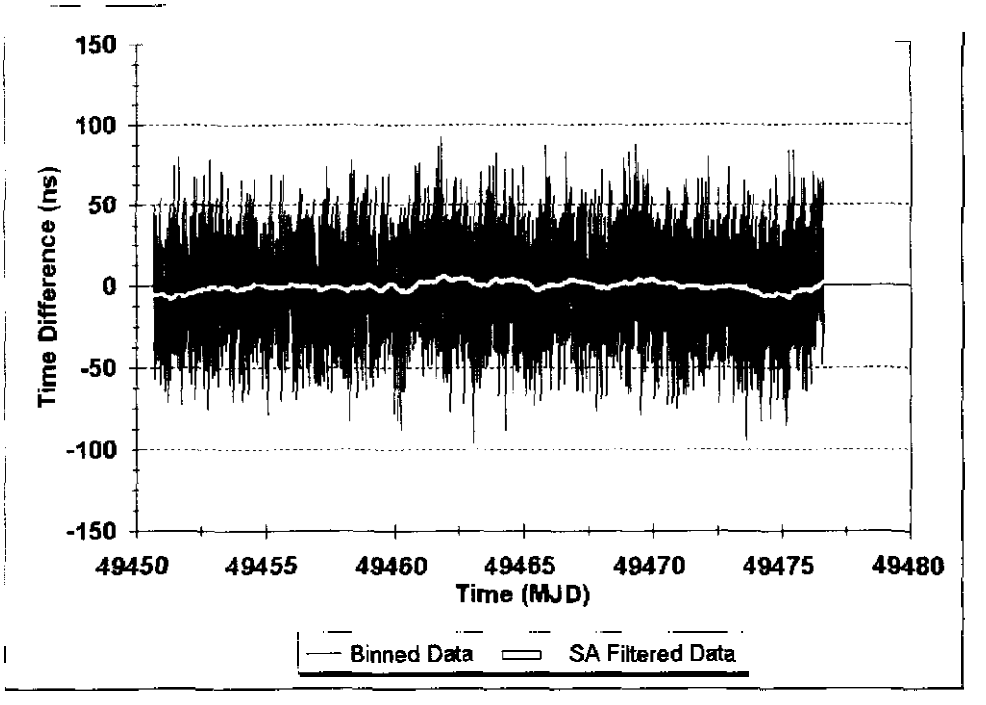

Figure 2. GPS vs. NIST Microstepper B -- 300 second binned data corrected for offset and slope.

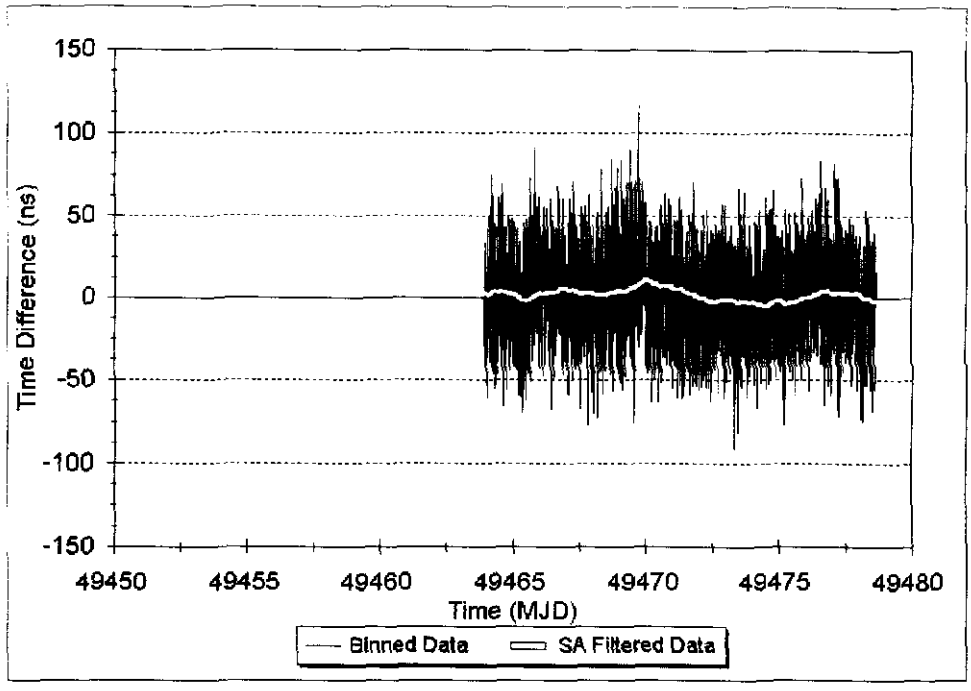

Figure 3. GPS vs. HPL HP5071A -- 300 second binned data

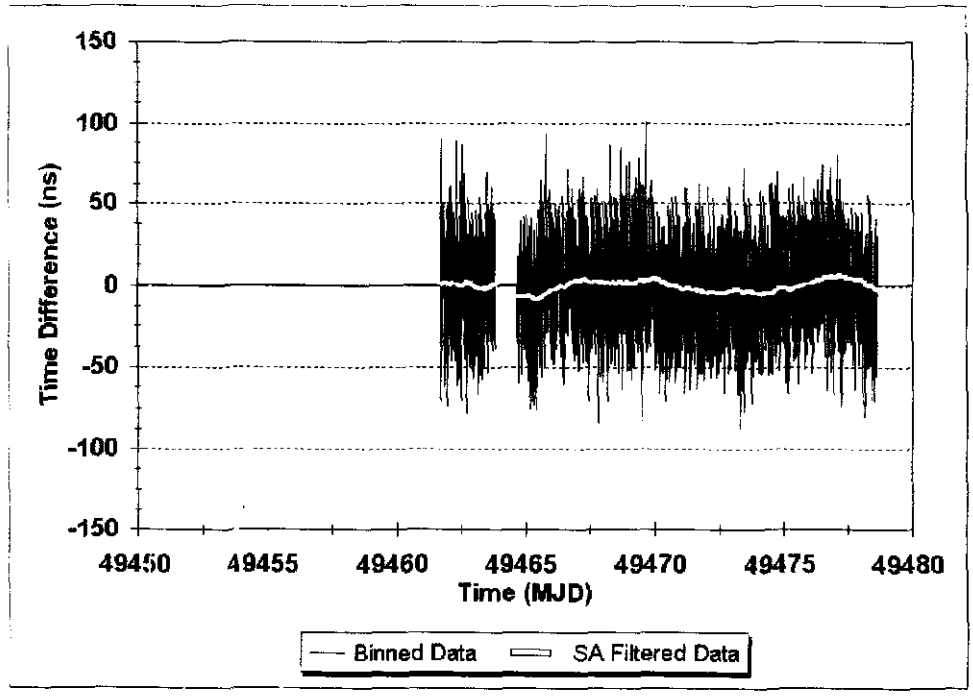

Figure 4. GPS vs SCD HP5071A Ensemble -- 300 second binned data corrected for offset and slope

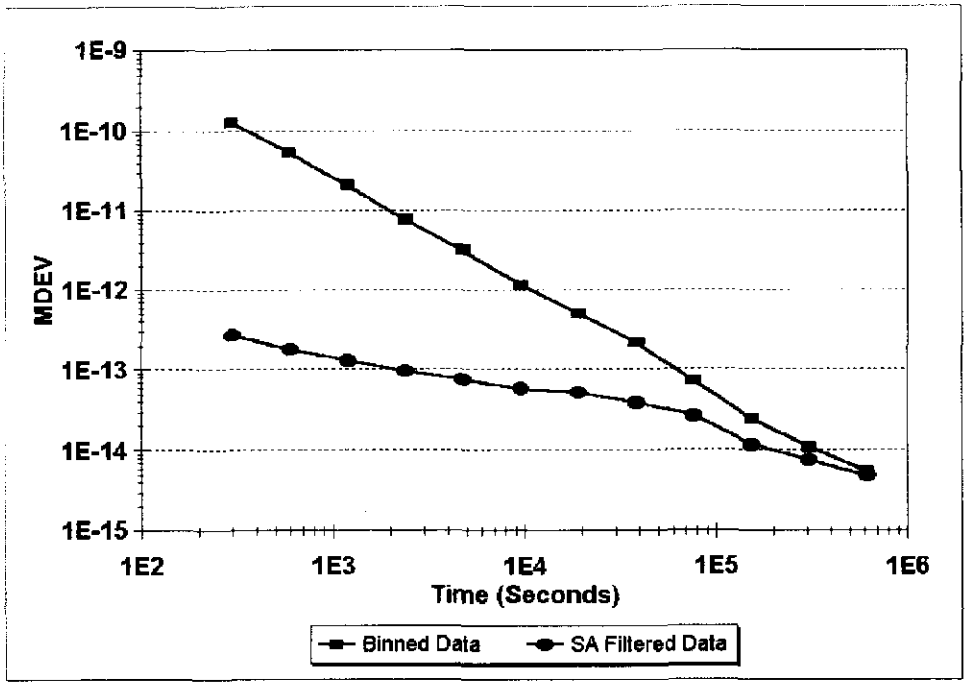

Figure 5. Modified Allan Variance, NIST Data

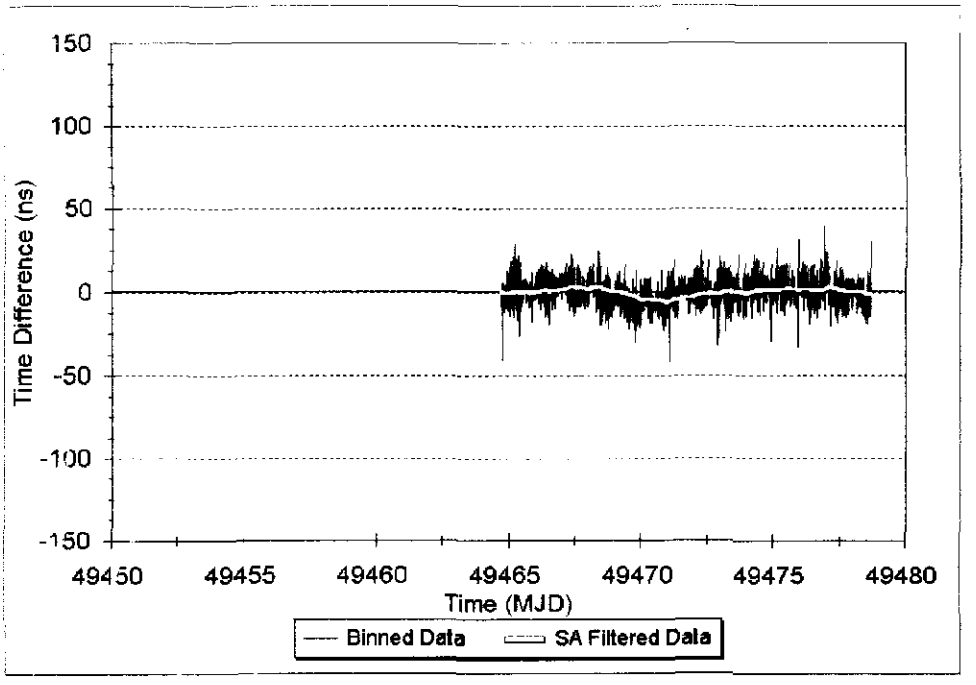

Figure 6. Difference data, SCD - HPL

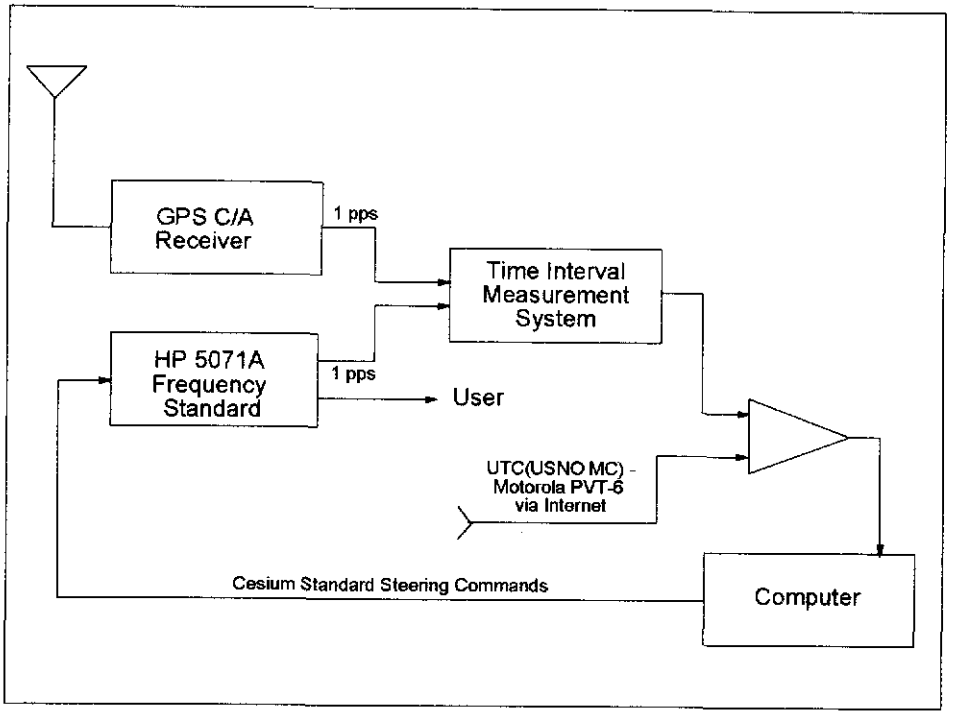

Figure 7. Block Diagram, GPS Disciplined Cesium Standard

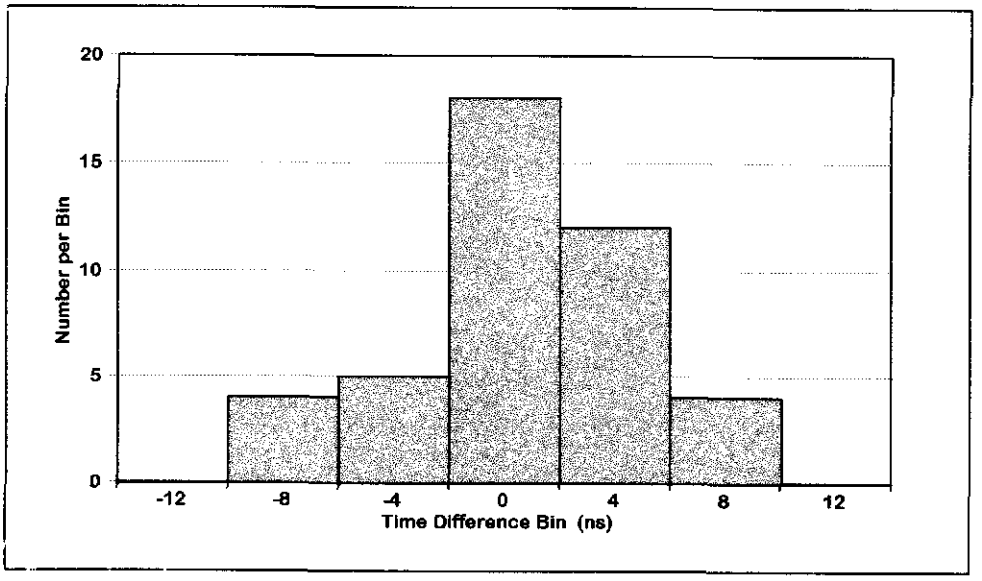

Figure 8. Histogram, HP5071A Disciplined to UTC(UISNO MC) Local Two-day Time Differences,

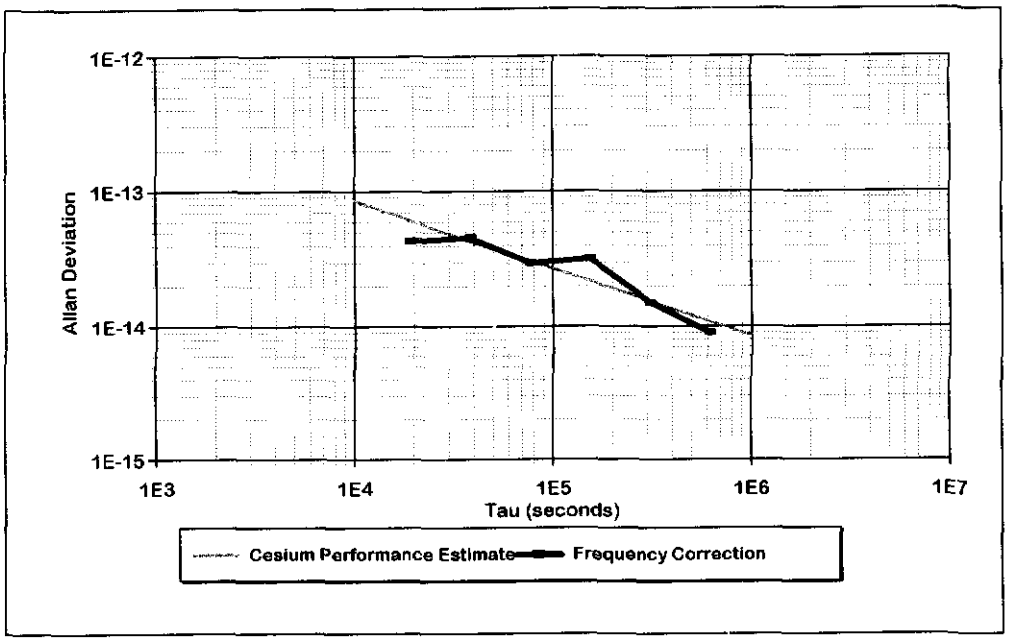

Figure 9. Allan Deviation, HP5071A Disciplined to UTC(USNO MC), steering data

	USNO	NIST	SCD	HPL
Offset (ns)		1146	579	571
Rate (ns/day)		1.8	8.9	-0.3
$\sigma_y(\tau=300$ sec) - original data	1.30×10^{-10}	1.28×10^{-10}	1.26×10^{-10}	1.26×10^{-10}
$\sigma_y(\tau=300$ sec) - filtered data	2.71×10^{-13}	2.69×10^{-13}	2.63×10^{-13}	2.63×10^{-13}

Table 1. Experimental Results, Part I

USNO -- NIST	0.67
NIST -- SCD	0.76
SCD -- HPL	0.96

Table 2. Normalized Cross-correlation Coefficients, Part I

FUNDAMENTAL CONCEPTS AND DEFINITIONS IN PM AND AM NOISE METROLOGY

Eva F. Pikal
NIST/University of Colorado

FUNDAMENTAL CONCEPTS

SIMPLE PM NOISE MEASUREMENT SYSTEMS

- TWO OSCILLATOR METHOD
- DELAY LINE
- CAVITY DISCRIMINATOR

SIMPLE AM NOISE MEASUREMENT SYSTEMS

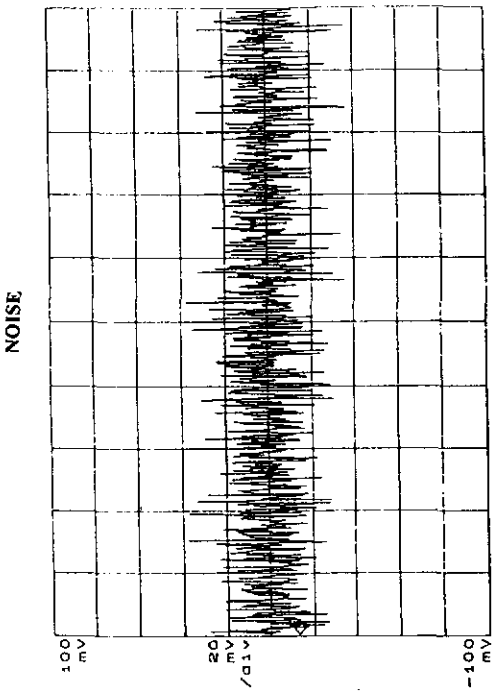

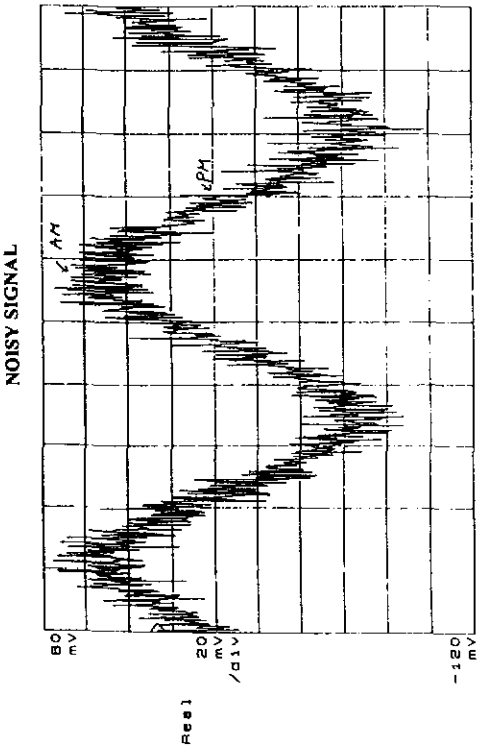

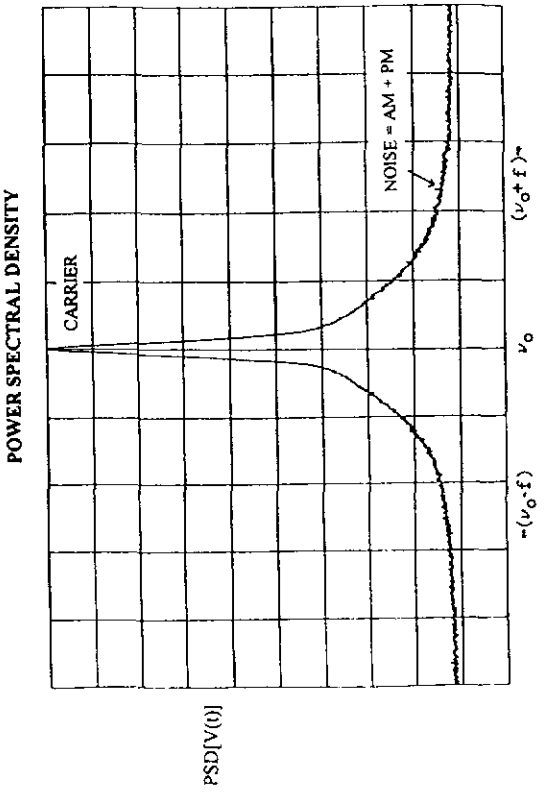

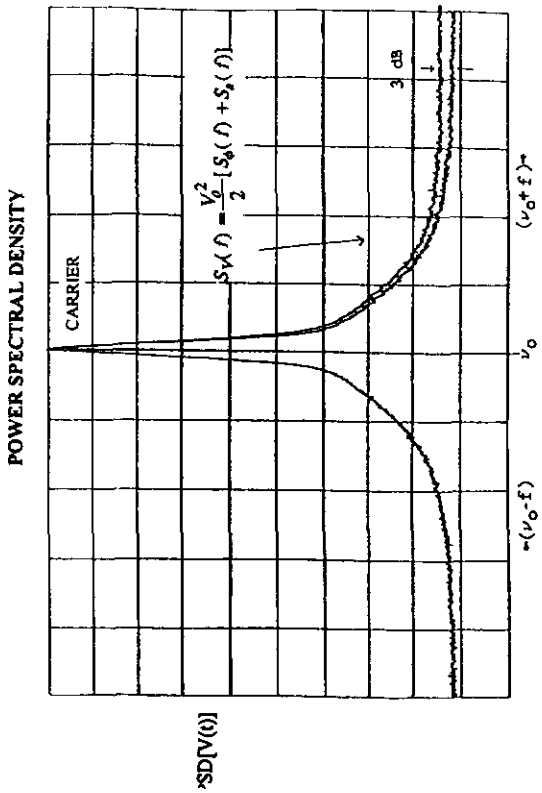

PHASE AND AMPLITUDE FLUCTUATIONS

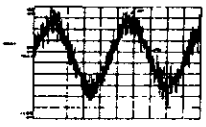

$$V(t) = [V_o + \varepsilon(t)]\cos(2\pi\nu_o t + \phi(t))$$

$$phase = 2\pi\nu_o t + \phi(t)$$

$$\omega(t) = \frac{d}{dt}[phase]$$

$$\nu(t) = \frac{1}{2\pi}\frac{d}{dt}[2\pi\nu_o t + \phi(t)]$$

$$\nu(t) = \nu_o + \frac{1}{2\pi}\frac{d}{dt}\phi(t)$$

Fractional frequency deviation:

$$y(t) = \frac{\nu(t) - \nu_o}{\nu_o} = \frac{1}{2\pi\nu_o}\frac{d}{dt}\phi(t)$$

WAVE THEORY REVIEW

perfect signal

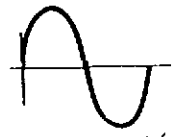

$$V(t) = V_o\cos(2\pi\nu_o t)$$

$$phase = 2\pi\nu_o t$$

$$T = period = 1/\nu_o$$

Fourier Transform:

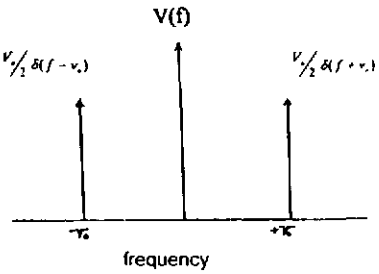

PHASE/AMPLITUDE NOISE RELATIONSHIPS

$$S_\phi(f) = [\Delta\phi(f)]^2\frac{1}{BW} \quad 0 < f < \infty \quad [\frac{rad^2}{Hz}]$$

$$S_\varepsilon(f) = \frac{[\Delta\varepsilon(f)]^2}{V_o^2}\frac{1}{BW} \quad 0 < f < \infty \quad [\frac{1}{Hz}]$$

$$y(t) = \frac{1}{2\pi\nu_o}\frac{d}{dt}\phi(t)$$

derivative in time = multiplication by ω in freq
= multiplication by ω^2 in spectral density

$$S_y(f) = \frac{1}{[2\pi\nu_o]^2}(2\pi f)^2 S_\phi(f)$$

$$S_\phi(f) = [\frac{\nu_o}{f}]^2 S_y(f) \quad 0 < f < \infty$$

$$S_\phi(f) = \mathcal{L}(\nu_o - f) + \mathcal{L}(\nu_o + f)$$

$\mathcal{L}(f)$

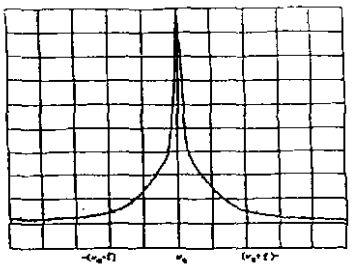

$$\mathcal{L}(f) = \frac{1}{2} S_\phi(f)$$

$$dBc/Hz = 10\log(\mathcal{L}(f))$$

RMS PHASE DEVIATION

$$\varphi^2(f)_{BW} = \int_{f-BW/2}^{f+BW/2} S_\varphi(f)df \ rad^2$$

POWER SPECTRAL DENSITY OF A NOISY SIGNAL

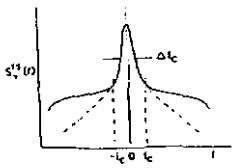

Double side-band spectral density:

$$S_V(f) \cong \frac{V_o^2}{2}[e^{-I(f_c)}\delta(f) + \quad S_\phi(f) + S_a(f)]$$

$$0 \le f \le \infty$$

$$I(f) = \int_{f_c}^{\infty} S_\phi(f)df$$

I(f) = integrated phase modulation due to pedestal

$\delta(f)$ = carrier with frequency $\pm f_c$

Power in carrier = $\frac{V_o^2}{2}e^{-I(f_c)} \approx \frac{V_o^2}{2}$ for $I(f_c) << 1$

FREQUENCY MULTIPLICATION/DIVISION EFFECTS ON PM NOISE

Frequency Multiplication

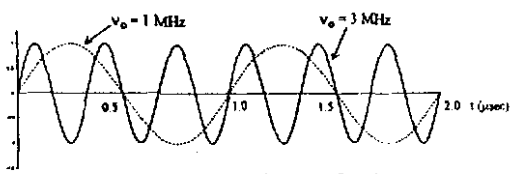

$$\nu_{o2} = N\nu_{o1} \qquad \Delta\phi_2 = N\Delta\phi_1$$

$$S_{\phi_2}(f) = \frac{[\Delta\phi_2]^2}{BW} = \frac{N^2\Delta\phi_1}{BW} = N^2 S_{\phi_1}(f)$$

FREQUENCY DIVISION:

$$\nu_{o2} = \frac{\nu_{o1}}{N}$$

$$S_{\phi_2}(f) = \frac{S_{\phi_1}(f)}{N^2}$$

FREQUENCY TRANSLATION

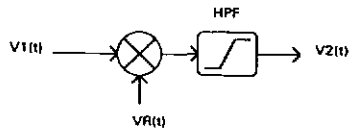

$$S_\phi(f,\upsilon_2) = S_\phi(f,\upsilon_1) + S_\phi(f,\upsilon_R) + S_{\phi T}(f)$$

WHERE $\upsilon_2 = \upsilon_1 + \upsilon_R$

$S_\phi(f,\upsilon_R)$ = PM NOISE OF REFERENCE SIGNAL

$S_{\phi T}(f)$ = PM NOISE ADDED BY THE TRANSLATOR

$S_\phi(f,\upsilon_2)$ DEPENDS ON THE DETAILS OF THE TRANSLATION

BASIC CONFIGURATIONS OF NOISE MEASUREMENTS

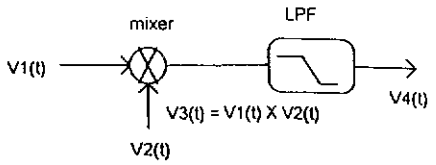

$$V_1(t) = [V_1 + \varepsilon_1(t)]\cos[2\pi\nu_o t + \phi_1]$$
$$V_2(t) = [V_2 + \varepsilon_2(t)]\cos[2\pi\nu_o t + \phi_2]$$

$$V_3(t) = \frac{A_1 A_2}{2}\{\cos[2\pi(2\nu_o)t + \phi_1 + \phi_2] + \cos[\phi_1 - \phi_2]\}$$

$$V_4(t) = \frac{A_1 A_2}{2}[\cos(\phi_1 - \phi_2)]$$

$$AM \Rightarrow \phi_1 - \phi_2 = \pi n$$

$$PM \Rightarrow \phi_1 - \phi_2 = \frac{\pi}{2} + \pi n$$

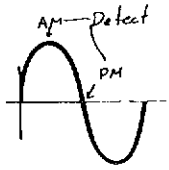

Simple PM Measurements

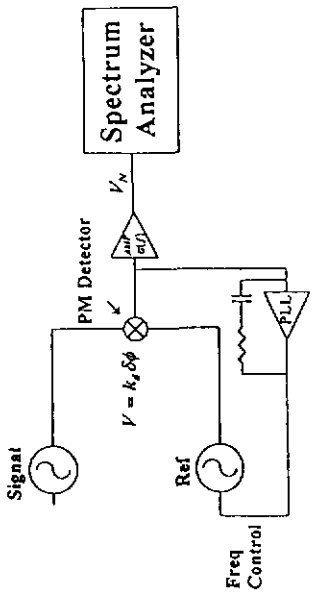

$\frac{PSDV_N}{[k_\phi G(f)]^2}$ measures $S_\phi(f)$ of the Signal plus the system noise.

It is difficult to seperate the system noise from a signal with low PM noise. Results uncorrected for PLL and gain variations with Fourier frequency.

NOISE TERMS INCLUDED IN $\frac{PSD(V_n)}{K_d^2 G(f)^2}$

$$S_\phi(f) = \frac{[\Delta\phi_A(f) - \Delta\phi_B(f)]^2}{BW} + \frac{V_n(f)^2_{mixer}}{K_d^2 BW} + \frac{V_n(f)^2_{amp}}{K_d^2 BW} + \frac{V_n(f)^2_{SA}}{K_d^2 G(f)^2 BW} + S_{\alpha A}(f)\beta_A^2 + S_{\alpha B}(f)\beta_B^2$$

$$S_\phi(f)_{pair} = S_{\phi A}(f) + S_{\phi B}(f) + \frac{V_n(f)^2_{system}}{K_d^2 BW} + S_{\alpha A}(f)\beta_A^2 + S_{\alpha B}(f)\beta_B^2$$

TO GET NOISE FLOOR SET A = B

$$S_\phi(f)_{Noise\ Floor} = (2\pi f \tau_{delay})^2 S_{\phi A}(f) + \frac{V_n(f)^2_{system}}{K_d^2 BW} + S_{\alpha A}(f)\beta_A^2 + S_\phi(f)_{power\ splitter}$$

$$\tau_{delay} = \frac{n\pi}{2}\frac{1}{\upsilon_o}$$

TO CALCULATE INDIVIDUAL PM NOISE FOR AN OSCILLATOR

$$S_\phi(f)_{AB} + S_\phi(f)_{AC} - S_\phi(f)_{BC} = 2S_{\phi A}(f) + \frac{V_n^2}{K_d^2 BW} + 2S_{\alpha A}(f)\beta_A^2$$

CALIBRATION FACTOR k_d

NOISE FLOOR IMPROVEMENT USING FREQUENCY MULTIPLIERS

DISCUSSION OF DIRECT PHASE COMPARISON

ADVANTAGES

HIGHEST RESOLUTION (LOWEST NOISE FLOOR)

NOISE FLOOR MEASURED WITH INFERIOR OSCILLATOR

VERY WIDE BAND PERFORMANCE

INEXPENSIVE

DISADVANTAGES

REQUIRES A REFERENCE OF COMPARABLE STABILITY

REQUIRES PHASE-LOCKED-LOOP (PLL) TO MAINTAIN $\delta\phi < 0.1$ rad

CALIBRATION DIFFICULT FOR $f << PLL\ BW$

SENSITIVE TO HARMONIC DISTORTION

FREQUENCY RESPONSE DEPENDS ON POWER & LOAD

DETERMINATION OF τ_d

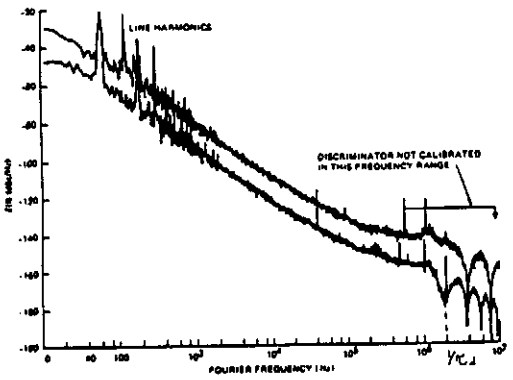

From: Infrared and Millimeter Waves, Vol. 11, pp 239-289, 1984 (also in NIST Technical Note 1337).

MEASUREMENT OF $S_\phi(f)$ USING A DELAY LINE

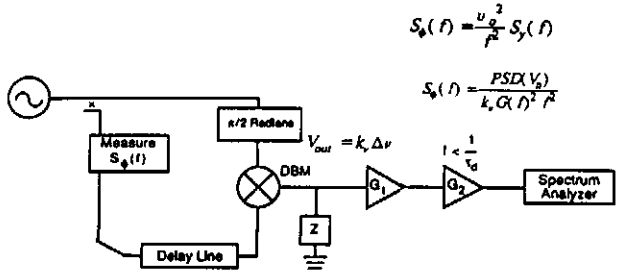

MEASUREMENT OF PHASE NOISE USING A HIGH-Q CAVITY

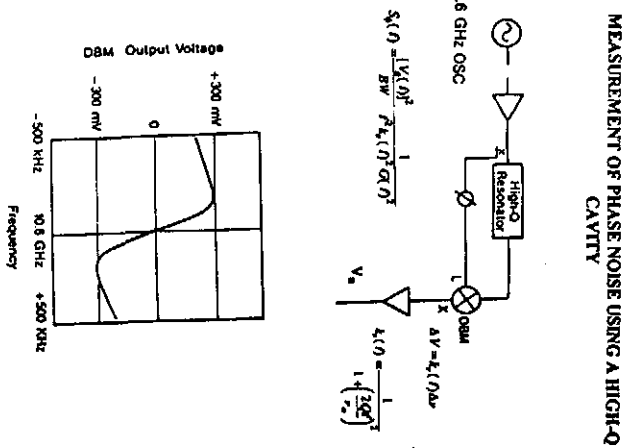

NOISE FLOOR COMPARISON FOR TWO MEASUREMENT SYSTEMS: DELAY LINE SYSTEM VS. TWO OSCILLATOR SYSTEM

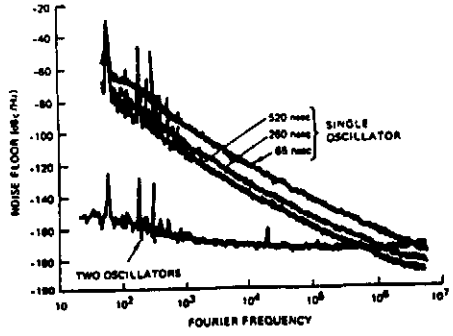

From: Infrared and Millimeter Waves, Vol. 11, pp. 239-289, 1984 (also in NIST Technical Note 1337).

DIRECT FREQUENCY COMPARISONS | **DIRECT PHASE COMPARISONS**

ADVANTAGES:

DOES NOT REQUIRE SECOND SOURCE	LOWEST NOISE FLOOR
SYSTEM TRACKS FREQUENCY CHANGES IN SOURCE	NOISE FLOOR MEASURED WITH INFERIOR OSCILLATOR
NO PLL EFFECTS	VERY WIDE BAND PERFORMANCE
SIMPLE CALIBRATION $V = G\,k\,\Delta\omega$	INEXPENSIVE

DISADVANTAGES:

NOISE FLOOR SCALES AS 1/f2 NEAR CARRIER	REFERENCE OF COMPARABLE STABILITY
NOISE FLOOR DIFFICULT TO MEASURE	REQUIRES PLL TO MAINTAIN $\Delta\phi < 0.1$ rad
DIFF. CAVITIES *REQUIRED FOR EACH* υ	CALIBRATION DIFFICULT FOR $f \ll$ PLL BW
DIFF. CAVITIES/DELAY LINES FOR DIFF. f	SENSITIVE TO HARMONIC DISTORTION
DIFFICULT TO MEASURE BEYOND CAVITY BW OR BEYOND DELAY LINE TIME	FREQUENCY RESPONSE DEPENDS ON POWER & LOAD

AM NOISE DEFINITION

$$S_a(f) = \left(\frac{\Delta\varepsilon}{V_o}\right)^2 \frac{1}{BW}$$

AM DETECTORS

Mixer Detector

Diode Detector

Simple AM Measurement

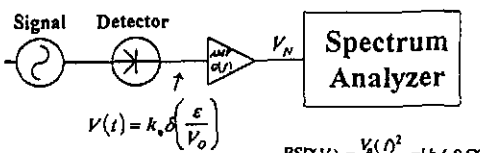

$\frac{PSDV_N}{[k_s G(f)]^2}$ measures $S_s(f)$ of the Signal plus the system noise.

It is difficult to seperate the system noise from a signal with low AM noise.

Determination of $[k_s(f)G(f)]$ for AM Measurement Systems

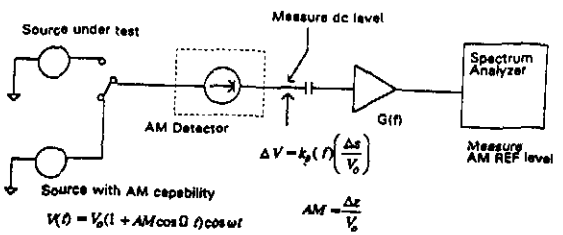

AM at the input signal: $\frac{1}{2}\left(\frac{\%AM}{100}\right)^2$ AM at output: AM REF level

$$[k_s(f)G(f)]^2 = \frac{\text{AM at Output}}{\text{AM at Input}} = \frac{(AM\ REF\ \text{level})^2}{\frac{1}{2}\left(\frac{\%AM}{100}\right)^2}$$